Plant Molecular Biology **56:** 225–239, 2004.

Identification of a novel plant MAR DNA binding protein localized on chromosomal surfaces

Satoru Fujimoto[1], Sachihiro Matsunaga[1], Masataka Yonemura[1], Susumu Uchiyama[1], Takachika Azuma[2] and Kiichi Fukui[1,*]

[1]*Department of Biotechnology, Graduate School of Engineering, Osaka University, 2-1, Yamadaoka, Suita, Osaka 565-0871, Japan (*author for correspondence; e-mail kfukui@bio.eng.osaka-u.ac.jp);* [2]*Research Institute for Biological Sciences (RIBS), Tokyo University of Science, 2669, Yamazaki, Noda, Chiba 278-0022, Japan*

Received 20 April 2004; accepted in revised form 14 September 2004

Key words: chromosomal surface, GFP, matrix-attachment region, nuclear matrix, visual screening

Abstract

We identified a novel nucleoplasm localized protein in *Arabidopsis* called AT-hook motif nuclear localized protein 1 (AHL1), which was isolated by visual screening of transformants using random GFP::cDNA fusions. AHL1 contains an AT-hook motif and unknown conserved PPC (plants and prokaryotes conserved) domain that includes a hydrophobic region. Approximately 30 paralogues were identified in the *Arabidopsis* genome. Proteins with PPC-like domains are found in Bacteria, Archaea and the plant kingdom, but in Bacteria and Archaea the PPC containing proteins of do not have an AT-hook motif. Thus, the PPC domain is evolutionary conserved and has a new function such as AT-rich DNA binding. AHL1 was mainly localized in the nucleoplasm, but little in the nucleolus and heterochromatic region, and was concentrated in the boundary region between euchromatin and heterochromatin. Biochemically, AHL1 was also found in the nuclear matrix fraction. In the M phase, AHL1 was localized on the chromosomal surface. The AT-hook motif was essential for matrix attachment region (MAR) binding, and the hydrophobic region of the PPC was indispensable for nuclear localization. Our results suggest that AHL1 is a novel plant MAR binding protein, which is related to the positioning of chromatin fibers in the nucleus by the presence of an AT-hook motif and PPC domain. In addition, AHL1 is located on the surface of chromosomes during mitosis.

Introduction

The total length of cellular DNA must be reduced approximately 10000-fold in the eukaryotic nucleus (reviewed by Pienta *et al*., 1991). Such condensation is achieved by elaborate DNA folding that involves interactions between DNA and a variety of proteins. The most commonly accepted model proposes a hierarchy of DNA organization within the nucleus. First, naked DNA is wound around histone octamers to form nucleosomes structured like 11 nm in diameter beads-on-a-string (Olins and Olins, 1974). Interactions between nucleosomal linker DNA and histone H1 generates a heterogeneously folded 30-nm long fiber structure (reviewed by van Holde and Zlatanova, 1995). This fiber structure is then organized into 5–200 kb-long loops, which become attached to a nuclear matrix or scaffold (Gasser and Laemmli, 1987). Anchorage of these loops to the nuclear matrix involves specific stretches of DNA termed matrix-attachment regions (MARs) (Mirkovitch *et al*., 1984).

The nuclear matrix is a structural framework that is involved in the architectural organization of the DNA network or the spatial positioning of chromatin in the eukaryotic nucleus. Biochemically, the nuclear matrix can be defined as the insoluble material that remains after removal of chromatin and soluble nuclear proteins (Berezney and Coffey, 1974). Electron microscopy revealed that matrices generally consist of a nuclear lamina and nuclear pore complexes surrounding an internal fibrogranular network of proteins and residual nucleolar proteins (He *et al*., 1990; Penman, 1995). A variety of proteins that interact with MARs have been identified in animals and include proteins that also have characteristic nuclear functions, such as maintenance of the genome stability related protein: DNA topoisomerase II (Adachi *et al*., 1989); architectural chromatin proteins: histone H1 (Izaurralde *et al*., 1989) and HMG-I/Y (Zhao *et al*., 1993); filament proteins: A- and B-type lamins, and NuMA (Ludérus *et al*., 1992, 1994); an RNA binding protein: hnRNP-U (Tsutsui *et al*., 1993; Fackelmayer *et al*., 1994; von Kries *et al*., 1994); and a tissue-specific transcription factor: SATB1 (Dickinson *et al*., 1992).

With the initiation of mitosis, the nuclear envelope is disrupted and the chromatin, which is confined to the nucleus during the interphase, becomes exposed to the cytoplasm and condenses into chromosomes. During mitosis, various nuclear matrix proteins show different localization patterns. Topoisomerase IIα distributes to the mid-rib of each chromatid, which corresponds to the chromosome scaffold throughout the prophase. During the metaphase, it becomes concentrated in the centromeric regions, and during the anaphase after segregation has occurred, this centromeric concentration of topoisomerase IIα disappears (Swedlow *et al*., 1993; Sumner, 1996). NuMA is localized on the spindle poles that ontribute to the formation and maintenance of focused microtubule arrays (Merdes *et al*., 1996). The lamins become hyperphosphorylated during mitosis as a result of their depolymerization. A-type lamins are partly dispersed as a soluble form throughout the mitotic cytosol and become partly chromosome-bound while the B-type lamins remain associated with the vesicles derived from the interphase nuclear membranes. At the end of mitosis, B-type lamins accumulate on the chromosomal surfaces during the late anaphase while A-type lamins reassemble on the nuclear envelopes during the G1 phase (Gerace and Blobel, 1980).

Plant nuclear matrices were thought to be morphologically similar to vertebrate matrices, and proteins antigenically related to animal nuclear matrix components have been reported in some plant species (McNulty and Saunders, 1992; Minguez and Moreno Diaz de la Espina, 1993; Yu and Moreno Diaz de la Espina, 1999). Recently, however, it has been suggested that plant nuclear matrices differ from vertebrate matrices. The fully sequenced *Arabidopsis* genome does not contain lamin-encoding genes or their homologues, suggesting that different proteins that play a similar role might have evolved to functionally replace those in the animal nuclear matrix. Some specific plant nuclear matrix proteins, such as two kinds of filament-like proteins, tomato MFP1 (Meier *et al*., 1996; Gindullis and Meier, 1999) and carrot NMCP1 (Masuda *et al*., 1997), and an MFP1-interacting protein, MAF1 (Gindullis *et al*., 1999) have been identified in the peripheral region of the plant nucleus. AHM1 was identified in the inner nuclear matrix of wheat (Morisawa *et al*., 2000), and two MAR binding proteins, MARBP-1 and MARBP-2, which have a significant homology to yeast nucleolar proteins, were found in the nuclear matrix of peas (Hatton and Gray, 1999). More recently, proteomic analysis of the *Arabidopsis* nuclear matrix was performed (Calikowski *et al*., 2003). In spite of these findings, our knowledge on the plant nuclear structure remains fragmentary because there has been no way to systematically search for these nuclear proteins.

In this study, we describe the characterization of a novel nuclear protein, AT-hook motif nuclear localized protein 1 (AHL1), which potentially functions as a connection between the nuclear framework and DNA of MAR sequences in interphase nuclei, and covers the chromosomes during mitosis.

Materials and methods

Visual screening of GFP::cDNA fusion transgenic seedlings

Visual screening was performed by modification of a method described by Cutler *et al*. (2000). CaMV35S-sGFP (S65T)-NOS3′ (Chiu *et al*.,

1996) was inserted into the multicloning sites of SpUC19, the ampicillin resistance gene (*β-lactamase*) of pUC19 has been replaced by the spectinomycine resistance gene (*aminoglycoside adenyltransferase*). The stop codon of the *GFP* was removed and the plasmid was renamed SpUCGFP. The CD4-14 cDNA library of *A. thaliana* was obtained from the Arabidopsis Biological Resource Center (Kieber *et al.*, 1993). The cDNA fragments in λ ZAP II were excited with ExAssist Interference-Resistant helper phage and *E. coli* SOLR (Stratagene) to generate phagemid vectors according to the manufacturer's instructions. The *Not*I digested cDNAs were ligated with *Not*I-digested SpUCGFP so that the cDNA was inserted under the sGFP gene. SpUCGFP-cDNA was digested with *Sse*8387I and ligated with *Sse*8387I-digested pEBis-kH2: pEBis-kH2 is a binary vector that has a kanamycin resistance (*neomycin phosphotransferase II*) and hygromycin resistance gene (*hygromycin B phosphotransferase*). The ligated populations were transformed into DH10B.

The floral dip method was used for *Agrobacterium*-mediated *Arabidopsis* transformation (Clough and Bent, 1998). *Agrobacterium tumefaciens* strain C58 (pMP90) was transformed with pEBis-kH2-containing GFP fusion genes by electroporation. Seeds taken from plants inoculated with *Agrobacterium* were germinated on MS agar containing 100 μg/ml of carbenicillin, 10 μg/ml of hygromycin and 50 μg/ml of kanamycin. Seedlings expressing GFP were screened with a fluorescence microscope (AxioPlan II, Carl Zeiss Jena, GmbH, Jena, Germany) equipped with a cooled charged-coupled device (CCD) camera (MicroMax, Roper Scientific Princeton Instruments, Trenton, NJ, USA).

A deconvolution method was used to obtain 3D images (Agard *et al.*, 1989). Plant images were captured with a cooled CCD camera (CH 350/L, Roper scientific Photometorics, Tucson, AZ, USA) using a fluorescence microscope (IX-70, Olympus, Tokyo Japan). In total, more than sixty 0.2-μm sections were collected from a cell. Initial data were analyzed using DeltaVision software (Applied Precision, LLC, Issaquah, WA, USA). Images were deconvoluted to obtain clear 3D images using a Deconvolution program then, projection images were generated using a Quick Projection or Volume Viewer program.

Construction of bacterial expression vectors

AHL1 cDNA was amplified from the *Arabidopsis* cDNA phagemid library using gene specific primers (AHL1-U: 5′-*CCATGG*TCTTAAATATGGAGT CTACCGG-3′, AHL1-R: 5′-*TGTACA*TGGAGT CTACCGGAGAAGCTG-3′). These primers contained additional *Nco*I and *Bam*HI sites as shown in italics, respectively. The resulting PCR product was cloned into pUC18, creating pUC-AHL1. The cDNA insert of AHL1 was recloned into pET-3d yielding pET-AHL1, which was used for recombinant AHL1 expression in *E. coli* BL21 (DE3).

To create an AHL1mut that disrupts the AT-hook motif, site-directed mutagenesis was performed by PCR with the following primers: primer sets AHL1-U and AHL1-ATR (5′-GGTCCATA CTTCCTTGCCGCTGCACGCTTCTTCTTCAT C-3′) and primer sets AHL1-R and AHL1-ATU (5′-GATGAAGAAGAAGCGTGCAGCGGCAA GGAAGTATGGACC-3′) were annealed with pUC-AHL1. Intermediated DNA fragments were produced by PCR and joined by PCR with the outer primers, AHL1-U and AHL1-R. The synthesized DNA was cloned into pUC18 then recloned into pET-3d yielding a pET-AHL1mut. Mutations were confirmed by DNA sequence analysis.

Overexpression and purification of AHL1

E. coli BL21 (DE3) carrying a recombinant plasmid was cultured in LB broth (100 μg/ml ampicillin) at 37 °C overnight. Four milliliteres of bacterial culture was then inoculated into 400 ml of LB broth (100 μg/ml ampicillin) and incubated at 37 °C with shaking. At an OD_{660} of 0.4, IPTG was added to a final concentration of 1 mM. After three hours incubation, the bacterial cells were harvested by centrifugation, and washed with and resuspended in 20 ml of sonication buffer (50 mM MES–KOH (pH 5.5), 300 mM NaCl, 1 mM DTT, and 1 mM PMSF). The cells were disrupted by sonication and the supernatants were obtained by centrifugation.

The soluble fraction was dialyzed against dialysis buffer A (20 mM MES–KOH (pH 5.5), 300 mM NaCl, 1 mM DTT and 1 mM PMSF) then absorbed into the matrix of the HiTrap SP column (Amersham Biosciences UK Ltd., Buckinghamshire, UK) and eluted with a

300–650 mM linear NaCl gradient. The eluted fraction was dialyzed against dialysis buffer B (20 mM MES–KOH (pH 5.5), 300 mM NaCl) and applied to a Superdex 200 Hiload 16/60 column (Amersham Biosciences) eluted with 120 ml of gel filtration buffer A (20 mM MES-KOH (pH 5.5), 300 mM NaCl).

Southwestern blot analysis

A 1.3 kb nucleotide sequence of *Arabidopsis* plastocyanin locus MAR-1 (PC-MAR1, accession number Z83321) (van Drunen *et al.,* 1997) and an 825 bp of full length *Arabidopsis* histone H1.1 gene (accession number P26568) were amplified from *Arabidopsis* genomic DNA and cloned into pUC18. PCR amplified fragments with the FITC-labeled primers 5′-GGAAACAGCTATGACCA TGATTAC-3′ and 5′-CCCAGTCACGACGTT GTAAAACGA-3′ were used as probes. The proteins were separated on 12% SDS polyacrylamide gels and transferred onto nitrocellulose membranes. DNA binding was performed in a DNA binding buffer containing 20 mM Tris–HCl, pH 7.5, and 150 mM NaCl with 10 ng/ml FITC-labeled DNA fragment in the presence of 10 μg/ml unlabeled synthetic oligonucleotides (Amersham Bioscience) as a competitor. After incubation for 12 h at room temperature, the membranes were washed with the DNA binding buffer and incubated with AP conjugated anti-FITC antibody (PerkinElmer Life Sciences, Inc.) in DNA binding buffer. The bands were detected using CDP-star (Amersham Bioscience).

Monoclonal antibody production

The recombinant AHL1 was injected into three Balb/c mice (100 μg per mouse). Initial injections were given subcutaneously with the immunogen adsorbed with alum, and killed *Bordetella pertussis*. Second injections were given subcutaneously with the proteins mixed with alum. Seven days after the second injection, two mice were injected intraperitoneally with 100 μg of AHL1 in PBS, three days before fusion. Spleen cells of these mice were fused with the myeloma cell line SP2/O and the resulting hybridoma cells were plated in 96-well plates. Two weeks after fusion, media from the wells showing cell growth were tested using ELISA. Monoclonal cell lines producing anti-AHL1 antibodies were identified and expanded in flasks to prepare large quantities of hybridoma supernatant.

Nuclei and nuclear matrix preparation

Nuclei isolations were performed according to the method of Xia *et al.* (1997) and Masuda *et al.* (1997) with some modifications. Fresh tissues were pulverized in liquid N_2 using a mortar and pestle. Pre-chilled Honda's buffer (2.5% Ficoll 400, 5.0% dextran T40, 0.4 M sucrose, 25 mM Tris–HCl (pH 7.5), and 10 mM $MgCl_2$, 10 mM β-mercaptoethanol and $1 \times$ Complete Protease Inhibitors (Roche)) was then added to the pulverized tissues and the homogenate was filtered through a 100- and 40-μm nylon mesh. Triton X-100 (5%) was added to the filtrate to a final concentration of 0.5% and stirred for 15 min on ice. This total extract was centrifuged at $1{,}500 \times g$ for 5 min then the pellet was washed with Honda's buffer containing 0.1% Triton X-100. The nuclei were subsequently purified by Percoll density gradient centrifugation. The pellet was resuspended in a resuspension buffer (0.4 M sucrose, 30% glycerol, 20 mM MES–KOH (pH 5.5), 10 mM KCl, 10 mM $MgCl_2$ and 0.1% Triton X-100) and the nuclei were layered on top of 15 ml Percoll A (30% Percoll, 0.4 M sucrose, 30% glycerol, 20 mM MES–KOH (pH 5.5), 10 mM KCl, 10 mM $MgCl_2$ and 0.1% Triton X-100) on 15 ml Percoll B (50% Percoll, 0.4 M sucrose, 30% glycerol, 20 mM MES–KOH (pH 5.5), 10 mM KCl, 10 mM $MgCl_2$ and 0.1% Triton X-100). The percoll gradient system was centrifuged at $8{,}000 \times g$ for 60 min and the interface of Percoll A and Percoll B was recovered from the tubes. The nuclear fraction was then mixed with an equal volume of resuspension buffer and the purified nuclei were collected by centrifugation at $5{,}000 \times g$ for 20 min.

High-salt extraction of the nuclear matrix was performed as described by Masuda *et al.* (1997). The nuclei were suspended in buffer A (50 mM MES, 5 mM $MgCl_2$, 0.25 M sucrose, and 10% glycerol, pH 6.0) plus 1 mM PMSF and incubated at 16 °C for 1 h with DNase I (SIGMA) at a final concentration of 50 μg/ml. After washing the nuclei three times, the salt concentration of the suspension was gradually increased to 1 M by adding an equal amount of buffer A containing 2 M

NaCl. The suspension was then incubated for 10 min on ice after which the nuclei were washed twice, and the final precipitant was used as the nuclear matrix.

Immunoblot analysis

A 1:1,000 dilution of anti-AHL1 culture supernatant and a 1:50 000 dilution of horseradish peroxidase-coupled anti-mouse secondary antibody (Sigma) were used to perform immunoblot analysis as described by Sambrook *et al.* (1989). Immunoreactive proteins on the protein gel blots were detected with the SuperSignal West Dura Chemiluminescent Substrate (Pierce).

Indirect immunofluorescence

Mouse anti-AHL1 monoclonal antibody and rabbit anti-dimethyl histone H3 (Lys4) (1:500, Upstate) polyclonal antiserum were used as the primary antibodies. Goat anti-mouse FITC (1:100, Leinco Technologies, Ins.) or goat anti-rabbit rhodamine (1:100, Jackson Immuno Research Laboratories) was applied as the secondary antibody. Root samples were prepared as described by Wako *et al.* (2002) with some modifications. The root tips were fixed in 4% (w/v) paraformaldehyde and macerated briefly with an enzyme mixture containing 2% (w/v) Cellulase Onozuka RS and 0.5% (w/v) Pectolyase Y-23. The samples were placed on glass slides and covered with cover slips, which were then tapped to allow the cells to spread. After freezing at − 80 °C the cover slips were removed and the slides were air dried at room temperature. The plasma membranes were then permeabilized with 0.1% Triton X-100 for 20 min. After washing, the samples were blocked with 1% BSA or 0.5% goat serum. They were then incubated with the primary antibody for 16 h at 4 °C in a humidified chamber. The slides were then washed and incubated with the secondary antibody for 3 h at 25 °C. After washing, the slides were counterstained with DAPI before mounting.

For image analysis, optical sections were obtained after producing deconvolution images. Linescans of the signal intensities of the voxels on a single line in the DAPI, FITC and rhodamine images were determined using Scion Image software (Scion Corporation). Further image processing and assembly were performed using Adobe Photoshop software (Adobe System, Mountain View, CA).

Expression of GFP fusion constructs of AHL1 and AHL1 deletion clones

To create GFP-AHL1 and AHL1-GFP plant expression vectors, AHL1 fragments were amplified by PCR using pUC-AHL1 as a template and the following primers: AHL1-U1 (5′-TGTACAT GGTCTTAAATATGGAGTC-3′) and AHL1-R1 (5′-GCGGCCGCTCAAGTTACATTGACATT-3′) for GFP-AHL1; and AHL1-U2 (5′-GTCGA CATGGTCTTAAATATGGAGTC-3′) and AHL1-R2 (5′-CCATGGTTACATTGACATT AATATCGC-3′) for AHL1-GFP. Using the internal restriction enzyme sites in the primers, the PCR products were recloned into the *Sal*I-*Nco*I or *Bsr*GI-*Not*I site of SpUCGFP. Fusion genes were digested with *Sse*8387I and ligated with *Sse*8387I-digested pEBis-kH2.

To create GFP-AHL1mut1, AHL1mut fragments were amplified by PCR using pUC-AHL1-mut as a template, and the primers AHL1-U1 and AHL1-R1. To create GFP-AHL1mut2, GFP-AHL1mut3 and GFP-AHL1mut4, AHL1 fragments were amplified by PCR using pUC-AHL1 as a template and the following primers: AHL1-U3 (5′ -TGTACAACGGGACTGTTGTAGCGTTATC-T -3′) and AHL1-R1 for GFP-AHL1mut2; AHL1-U1 and AHL1-R4 (5′-GCGGCCGCTCACG CTAAAAAACTTCCTAC-3′) for GFP-AHL 1mut3; and AHL1-U1 and AHL1-R3 (5′-GCGGCCGCTCAACCGGCGAGGCCACCG CC-3′) for GFP-AHL1mut4. Other procedures were the same as those used during the construction of the GFP-AHL1 plant expression vector.

Transformation of GFP-AHL1 into tobacco BY-2

Transformation of the tobacco BY-2 suspension-cultured cells was performed with the *Agrobacterium* mediated method as described previously (An, 1987). The fusion genes were inserted into the T-DNA region of the binary vector pEBis-kH2. *Agrobacterium* strain EHA101 (Hood *et al.*, 1986) was transformed with the binary vector by electroporation. *Agrobacterium* was co-cultivated with BY-2 cells in 9-cm Petri dishes for 48 h at 25 °C.

The co-culture was then harvested and transferred to a selective medium containing hygromycin and carbenicillin for selection.

Results

Identification of AHL1 with visual screening using a random GFP::cDNA fusions method

We isolated a novel nucleoplasm localized protein in *Arabidopsis* by visual screening of transformants using random GFP::cDNA fusions. Figure 1 shows the fluorescence distribution pattern of the isolated line: the fusion protein is localized in the nucleoplasm (Figure 1B). Figure 2A shows the deduced amino acid sequence of the cDNA (At4g12080, NP_192945): the gene consisted of five exons. The endogenous protein contained 356-amino acids with a calculated molecular mass of 37 kDa and a pI of 9.94. It was also predicted to contain an AT-hook motif and a conserved domain, plants and prokaryotes conserved (PPC) domain, which was described as DUF296 (domain of unknown function 296) in InterPro (http://www.ebi.ac.uk/interpro/) (Figure 2A). This protein was referred to as AHL1 (AT-hook motif nuclear localized protein 1). In *A. thaliana*, approximately 30 genes were observed as having significant similarities with *AHL1* at the amino acid level in the haploid genome (Arabidopsis Genome Initiative, 2000) (Figure 2C). Fourteen paralogues showed an especially high similarity to AHL1 (Figure 2C). A number of homologues of the primary amino acid sequence of AHL1 were also observed in plants such as *Oryza sativa* (KOME; http://cdna01.dna.affrc.go.jp/cDNA/) (Kikuchi *et al.*, 2003), *Zea mays*, and *Pisum sativum* (Figure 2B). Almost all the homologues have one or two AT-hook motifs and a conserved PPC domain in the mid to C-terminal portion. However, there are no proteins with a PPC domain in animals or fungi. In many prokaryotes, there are functionally unknown single copy proteins with PPC but without an AT-hook motif (Figure 2D).

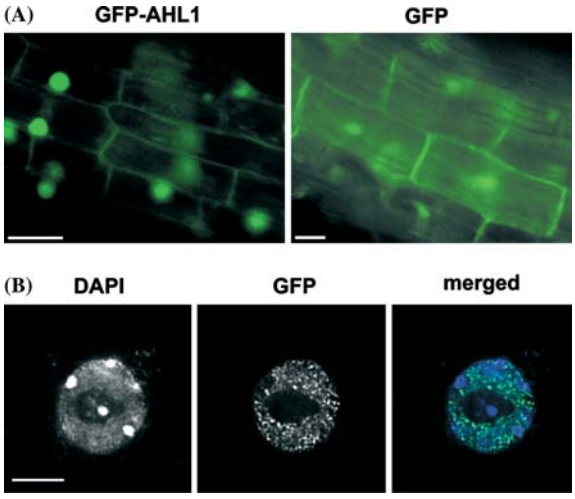

Figure 1. Subcellular localization of GFP-AHL1 in *Arabidopsis*. (A) Fluorescence distribution pattern of GFP-AHL1 in *Arabidopsis* root cells (left). The right image indicates the fluorescence distribution pattern of GFP. Scale bars = 20 μm. (B) Subnuclear distribution of GFP-AHL1 in *Arabidopsis* root cells. Sectioned images after deconvolution of DAPI fluorescence (left) and GFP-derived fluorescent emission images (middle). The right image indicates the merged image. Scale bar = 5 μm.

Association of AHL1 with MARs through the AT-hook motif in vitro

To confirm the DNA binding ability and determine the binding specificity of AHL1, a DNA binding assay was performed using a Southwestern blot assay. AHL1 was expressed in *E. coli* as a native form protein and recombinant AHL1 was expressed in both soluble and insoluble fractions. The full length AHL1 was purified from the soluble fraction using ion-exchange chromatography and gel filtration chromatography (Figure 3A), and was used for an *in vitro* DNA binding assay. The plastocyanin locus MAR-1 (PC-MAR1) (van Drunen *et al.,* 1997) and histone H1 genes of *A. thaliana* were used as probes for the MAR DNA and non-MAR DNA, respectively. As shown in Figure 3B, AHL1 was able to bind with the MAR sequence in the presence of poly (dI-dC)-poly (dI-dC). In contrast, when non-MAR DNA was used as a probe, the binding capability of AHL1 was competed with by poly (dI-dC)-poly (dI-dC).

The interaction between the AT rich DNA sequence in the MAR sequence and AHL1 was examined by the addition of poly (dA-dT)-poly (dA-dT) as an unlabelled competitor. Figure 3 shows that poly (dA-dT)-poly (dA-dT) inhibited MAR DNA from binding to AHL1. An interaction between the AT-hook motif and MAR sequence was confirmed by replacing the conserved

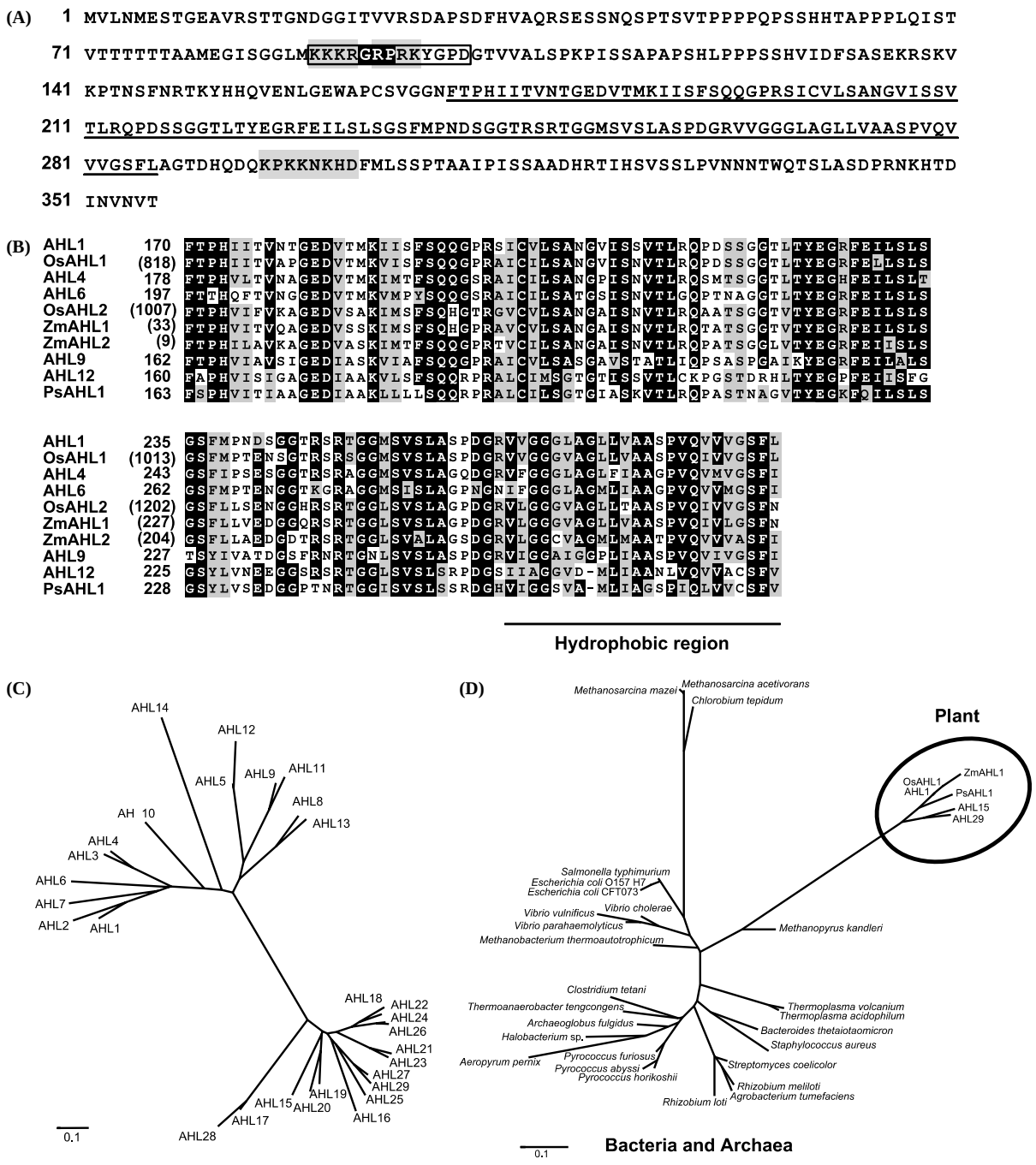

tripeptide sequence of glycine-arginine-proline in the AT-hook motif with an alanine tripeptide. The three conserved residues in HMG I/Y were previously shown to directly participate in the interactions with DNA (Huth *et al*., 1997). The mutant protein, Mut1, without this conserved sequence showed much less DNA binding activity (Figure 3B). Therefore, the AT-hook motif seems to be essential for the binding of AHL1 to MAR suggesting that AHL1 is a binding protein that binds to MAR and the AT-rich sequence through the AT-hook motif.

Localization of endogenous AHL1 in the nuclear matrix during the interphase and in the chromosomal surface region during the M phase

A monoclonal antibody against AHL1 was prepared using mice with purified recombinant AHL1 and named mAb12b. The reactivity of mAb12b against recombinant AHL1 was confirmed (data not shown). The nuclear matrix was prepared from whole tissues using a high-salt extraction method, and the interaction of AHL1 with the nuclear matrix was examined. Figure 4A shows that mAb12b recognized a 37-kDa AHL1 band in the nuclear extract and nuclear matrix fraction but not in the soluble protein fraction.

The nuclear localization of AHL1 was confirmed by immunofluorescence microscopy. As shown in Figure 4B, when permeabilized root cells of seedlings were incubated sequentially with mAb12b and a FITC-conjugated secondary antibody, a green signal was observed mainly in the nucleoplasm in a scattered distribution, but little in the DAPI-bright heterochromatic chromocenters during interphase. This distribution pattern was consistent with that of the GFP fusion protein (Figure 1B). During mitosis, the antigen was observed on the surface region of the chromosomes by deconvolution microscopy. Chromosomal surface localization was observed from the prophase to the telophase therefore, showing that AHL1 was localized specifically on the chromosomal surface region throughout mitosis.

The localization pattern of AHL1 was compared with the DNA condensation revealed by DAPI staining and immunostaining of methylated lysine 4 in histone H3 (MtK4H3) (Figure 5). In *A. thaliana*, it was reported that immunosignals for MtK4H3 are enriched in euchromatin, but they are not detected in nucleoli or heterochromatic chromocenters (Houben *et al.*, 2003). During mitosis, MtK4H3 was distributed on the chromosomes. Figure 5C shows the signal intensity of AHL1. During the interphase, AHL1 is not precisely co-localized with MtK4H3-euchromatin but was abundant at the boundary between DAPI positive heterochromatins and MtK4H3 positive euchromatin.

The hydrophobic region of the PPC is essential for nuclear localization

To determine the essential domain required for nuclear and/or chromosomal AHL1 localization, the expression of GFP-AHL1 and deletion mutants of the GFP-AHL1 domains in tobacco BY-2 cells was examined. Figure 6 illustrates the localization of the fusion proteins used for these experiments. N- and C-terminal fusion of AHL1

Figure 2. Amino acid sequence of AHL1. (A) Amino acid sequence of AHL1 deduced from the nucleotide sequence. The AT-hook motif (89–101) is boxed; conserved amino acids in the AT-hook motif are highlighted in black; the PPC (170–286) is underlined; and the NLSs (89–92, 94–97 and 295–302) are boxed in grey (Genbank accession number: NP_192945). (B) Alignment of amino acid sequence homologues. Ten PPC sequences from four plant species were aligned. Amino acid positions from the N-terminal are shown after the protein names. Hypothetical protein sequences without GenBank accession numbers are indicated with their nucleotide positions in parentheses. The solid and shaded boxes represent identical and similar amino acid residues, respectively. (GenBank accession numbers: AHL4 (At5g51590), NP_199972; AHL6 (At5g62260), NP_201032; AHL9 (At2g45850), NP_182109; AHL12 (At1g63480), NP_176537; *Oryza sativa* AHL1 (OsAHL1), AK068379; *Oryza sativa* AHL2 (OsAHL2), AK105419; *Zea mays* AHL1 (ZmAHL1), AY106980; *Zea mays* AHL2 (ZmAHL2), AY105124; *Pisum sativum* AHL1 (PsAHL1), T06584). (C) Phylogenetic tree of the *Arabidopsis* AHL1 homologues. (GenBank accession numbers: AHL2 (At4g22770), NP_194008; AHL3 (At4g25320), NP_194262; AHL5 (At1g63470), NP_176536; AHL7 (At4g00200), NP_191931; AHL8 (At5g46640), NP_199476; AHL10 (At2g33620), NP_565769; AHL11 (At3g61310), NP_191690; AHL13 (At4g17950), NP_567546; AHL14 (At3g04590), NP_187109; AHL15 (At3g55560), NP_191115; AHL16 (At2g42940), NP_181822; AHL17 (At5g49700), NP_199781; AHL18 (At3g60870), NP_191646; AHL19 (At3g04570), NP_566232; AHL20 (At4g14465), NP_567432; AHL21 (At2g35270), NP_181070; AHL22 (At2g45430), NP_182067; AHL23 (At4g17800), NP_193515; AHL24 (At4g22810), NP_194012; AHL25 (At4g35390), NP_195265; AHL26 (At4g12050), NP_192942; AHL27 (At1g20900), NP_173514; AHL28 (At1g14490), NP_172901; AHL29 (At1g76500), NP_177776. (D) Phylogenetic tree of the PPC from plant AHL1 homologues and prokaryotic PPC proteins. GenBank accession numbers: *Aeropyrum pernix*, BAA80508; *Agrobacterium tumefaciens*, AAL44941; *Archaeoglobus fulgidus*, AAB91134; *Bacteroides thetaiotaomicron*, AAO76223; *Chlorobium tepidum*, AAM71944; *Clostridium tetani*, AAO35778; *Escherichia coli* CFT073, AAN81954; *Escherichia coli* O157:H7, AAG58054; *Halobacterium* sp., AAG20444; *Methanobacterium thermoautotrophicum*, AAB85719; *Methanopyrus kandleri*, AAM01827; *Methanosarcina acetivorans*, AAM05077; *M. mazei*, AAM32530; *Pyrococcus abyssi*, CAB50172; *P. furiosus*, AAL80743; *P. horikoshii*, BAA29895; *Rhizobium loti*, BAB53068; *R. meliloti*, CAC48467; *Salmonella typhimurium*, AAL21946; *Staphylococcus aureus*, BAB56856; *Streptomyces coelicolor*, CAB62688; *Thermoanaerobacter tengcongensis*, AAM23579; *Thermoplasma acidophilum*, CAC12014; *T. volcanium*, BAB60149; *Vibrio cholerae*, AAF96489; *V. parahaemolyticus*, BAC62396; *V. vulnificus*, AAO07403.

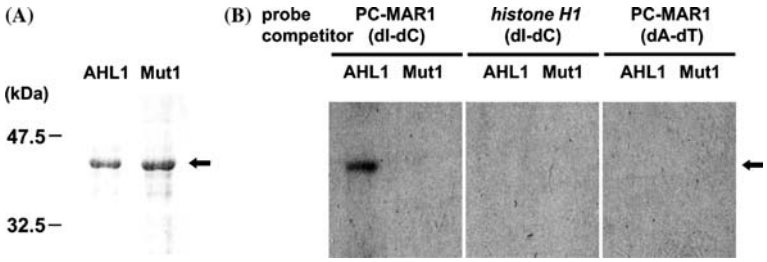

Figure 3. DNA binding properties of AHL1 *in vitro*. (A) Recombinant AHL1 and AHL1mut1 proteins in *E. coli*. Purified proteins were separated on a 12% SDS-polyacrylamide gel and visualized with Coomassie blue staining. The numbers on the left indicate the size in kilodaltons of the molecular mass markers. The arrow indicates the position of AHL1. (B) Recombinant proteins were blotted onto nitrocellulose and binding assays were performed with the following probes: fluorescein-labeled plastocyanin locus MAR-1 (PC-MAR1) for MAR DNA and *histone H1* for non-MAR DNA, and detected with CDP star. AT contents of PC-MAR1 and *histone H1* were 71% and 49%, respectively. dI-dC and dA-dT mean containing of 10 μg/ml competitors of poly (dI-dC)-poly (dI-dC) or poly (dA-dT)-poly (dA-dT). The arrow indicates the position of AHL1.

to the GFP, and C-terminal fusion of AHL1 mutants were constructed. Unfused GFP was used as a control. In GFP-AHL1mut1, glycine-arginine-proline, conserved amino acids of the AT-hook motif were replaced by three alanines. In GFP-AHL1mut2, an upstream region containing the AT-hook motif was deleted; in GFP-AHL1mut3, a downstream of the hydrophobic region was deleted; and in GFP-AHL1mut4, a downstream region containing the hydrophobic region of the PPC was deleted. AHL1 has two putative nuclear localization signals (NLSs) in the AT-hook motif (amino acid residues 89–92 and 94–97) and two NLSs in the downstream region of the PPC (295–298 and 296–302) (http://psort.nibb.ac.jp/) (Nakai and Kanehisa, 1992). GFP-AHL1mut1 lost one NLS, and GFP-AHL1mut2, GFP-AHL1mut3 and GFP-AHL1-mut4 lost two NLSs (Figure 6).

Figure 6 also shows the localization of GFP-AHL1, GFP-AHL1mut1 and GFP-AHL1mut2 in the nuclei during the interphase. It is thought that the AT-hook motif containing the upstream region is not essential for nuclear localization. Although GFP-AHL1mut3 also localized mainly in the nuclei, a portion of the fusion protein was diffused in the cytoplasm. GFP-AHL1mut4 was not localized in the nuclei but a small amount of signal was localized in the cytoplasm. These data indicate that the AT-hook motif and downstream region of the PPC are not very effectively localized in the nucleus, but that the hydrophobic domain in the PPC itself is essential for nuclear localization.

Discussion

In this study, we used visual screening to identify a novel protein, AHL1, which localizes in the nuclei. AHL1 consists of two characteristic domains, an AT-hook motif and PPC domain. In the *Arabidopsis* genome, approximately 30 paralogues were identified. AHL1 proteins also have a number of homologues in various plants such as rice, maize and garden peas. The PPC domain is the first domain to be identified that is evolutionary conserved in Bacteria, Archaea and the plant kingdom but not in other Eukarya. The amino acid sequence of a large subunit of ribulose bisphosphate carboxylase/oxygenase (RuBisCO) is also conserved in plants, photosynthetic bacteria, non-photosynthetic bacteria and Archaea (Ashida *et al.,* 2003). In the non-photosynthetic bacteria *Bacillus subtilis*, this RuBisCO-like protein catalyzes the 2,3-diketo-5-methylthiopentyl-1-phosphate enolase reaction during the methionine salvage pathway (Ashida *et al.,* 2003). Thus it is likely that the PPC domain, like RuBisCO, plays an essential role in plants.

It is worth noting that no prokaryotic PPC has a stretch that includes an AT-hook motif. The AT-hook motif is a short DNA binding protein motif which was first described in the high mobility group non-histone chromosomal proteins, HMG-I/Y (Reeves and Nissen, 1990). The AT-hook motif is known to interact with the minor groove of AT-rich sequences (Huth *et al*., 1997). It has also been observed in other DNA binding proteins from a wide range of animals and microorganisms

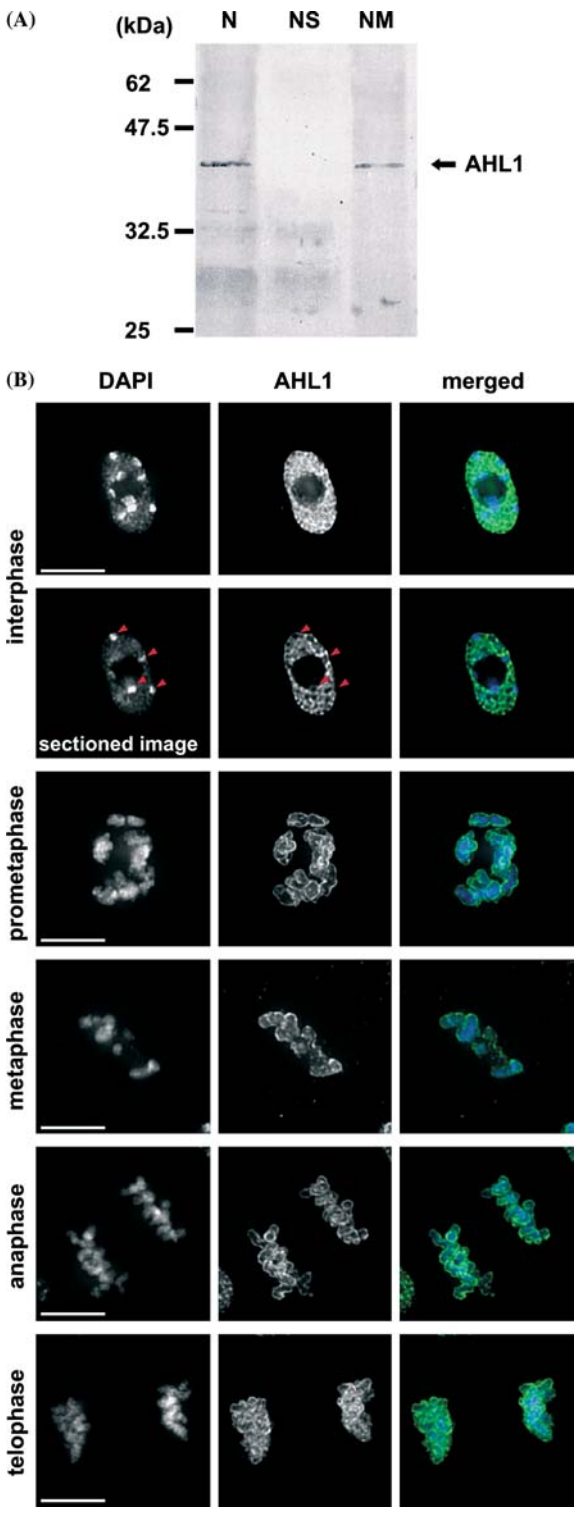

Figure 4. Presence of AHL1 in the nuclear matrix and is localized on the chromosome surfaces during mitosis. (A) *Arabidopsis* total nuclear proteins (N), nuclear proteins solubilized during the high-salt treatment (NS) and nuclear matrix proteins (NM) were separated on 12% SDS-polyacrylamide gels. Immunodetection was conducted using the anti-AHL1 antibody. The arrow indicates the position of AHL1. (B) Subcellular localization of AHL1 during the cell cycle in squashed *Arabidopsis* root cells. Immunolabeling of the root cells was conducted with mAb12b. The left column shows DNA staining with DAPI the middle column shows AHL1 and the right column shows merged images. AHL1 and DAPI are shown in green and blue, respectively. The red arrowheads indicate DAPI-positive chromocenters and the second line indicates the sectioned images after deconvolution. The other lines indicate the projection images after deconvolution. Scale bars = 5 μm.

(Aravind and Landsman, 1998). Unlike the several well-characterized DNA binding motifs, the AT-hook motif is short and has a typical tripeptide pattern with a glycine-arginine-proline at its center. PPC contains a hydrophobic region in the C terminal, and in the case of plants, is often found in several proteins with the AT-hook motif. Characterization of the DNA binding properties *in vitro* indicates that AHL1 binds to the AT-rich DNA sequence in the MAR sequence with high affinity using the AT-hook motif. Because Archaeal histones do not possess the N-terminal tail region of the eukaryotic histone, the eukaryotic histone is thought to have obtained its new function through acquisition of the N-terminal tail. The N-terminal regions of histone proteins play significant roles by modifying histone proteins during various cellular functions after translation (Strahl and Allis, 2000). Like the N-terminal tail of the eukaryote histone, a unique function of plant AHL1 must occur in plant nuclei with the addition of an AT-rich DNA binding capability.

Analysis of the primary amino acid sequence revealed that AHL1 has no coiled-coil structure or repeated sequences. Such structural features are found in filament proteins such as MFP (Meier *et al*., 1996) and NMCP1 (Masuda *et al*., 1997). However, nuclear matrix extraction under high salt conditions followed by immunodetection of AHL1 using mAb12b indicated that the defined nuclear matrix fraction contains AHL1. Therefore AHL1 does not seem to serve as an architecture component of the nuclear matrix, but might be involved in specific nuclear functions that are related to nuclear architecture–MAR interactions. The hydrophobic region of the PPC

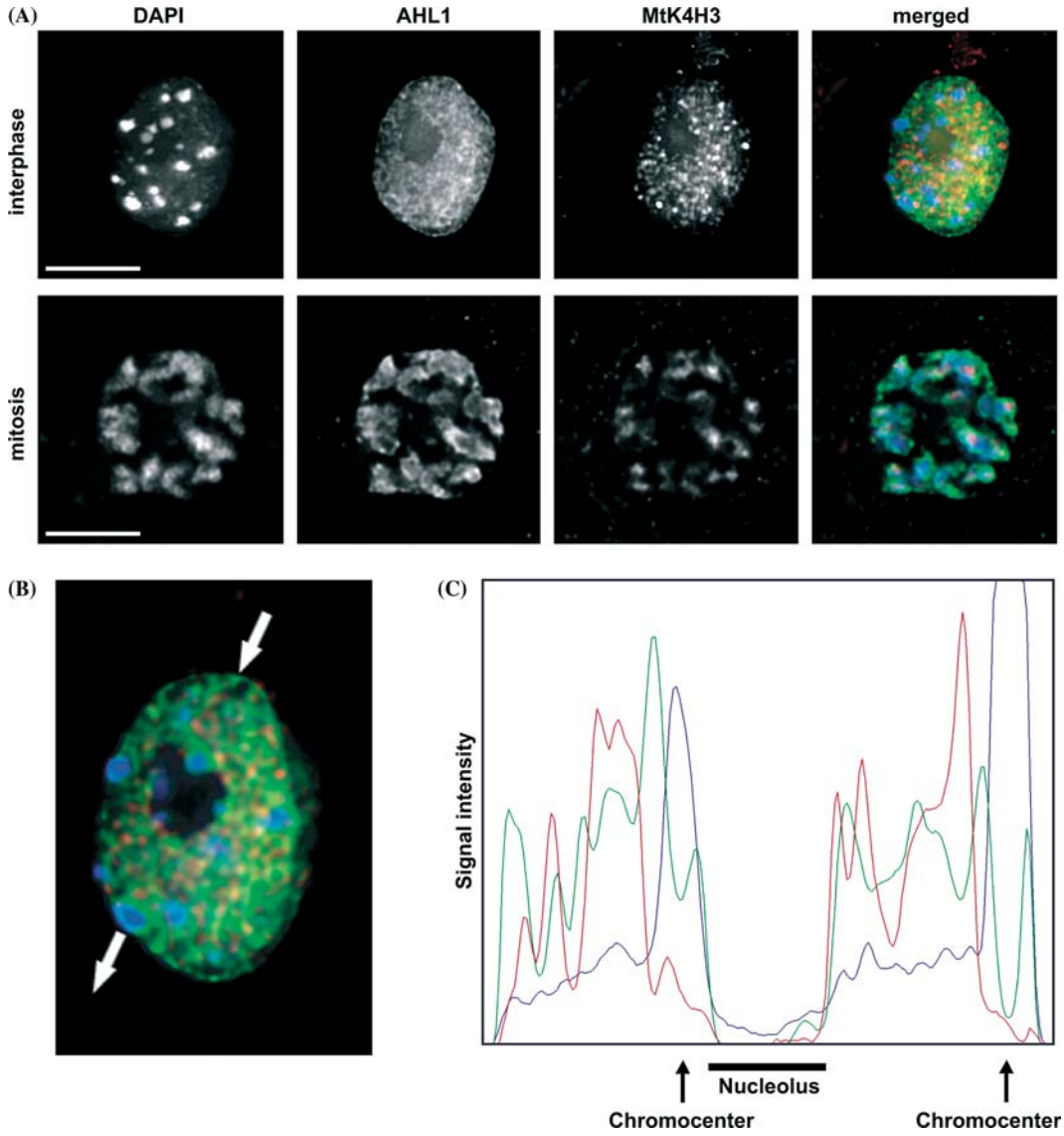

Figure 5. Localization of MtK4H3 and AHL1 in *Arabidopsis* root cells. (A) Triple staining of interphase and mitotic cells for DNA, AHL1 and MtK4H3. The first column shows DNA staining with DAPI the second column shows immunostaining of AHL1 the third column shows immunostaining of MtK4H3 and the last column shows merged images. DAPI, AHL1 and MtK4H3 are shown in blue, green and red, respectively. These images represent projection images after deconvolution. (B and C) The fluorescent intensity of the lines between the arrows in (B) was analyzed as shown in (C). The blue, green and red lines represent the DAPI fluorescence of DNA intensity, the FITC fluorescence of AHL1, and the rhodamine fluorescence of MtK4H3, respectively. The black arrows indicate DAPI-positive heterochromatin and the lower black line indicates the nucleolus. Scale bars = 5 μm.

of AHL1 is essential for nuclear localization of these proteins. A similar phenomenon is known in the plant MAR binding protein MFP the hydrophobic N-terminus of which is essential for its correct localization (Gindullis and Meier, 1999). Thus it is quite probable that the hydrophobic region is one of the important domains for the localization of plant MAR binding proteins in the nuclear matrix.

AHL1 was localized in the nucleoplasm in a scattered distribution and was AHL1 scarcely localized in DAPI-positive chromocentric regions. Similar distribution patterns have been reported for the plant internal nuclear matrix-localized protein,

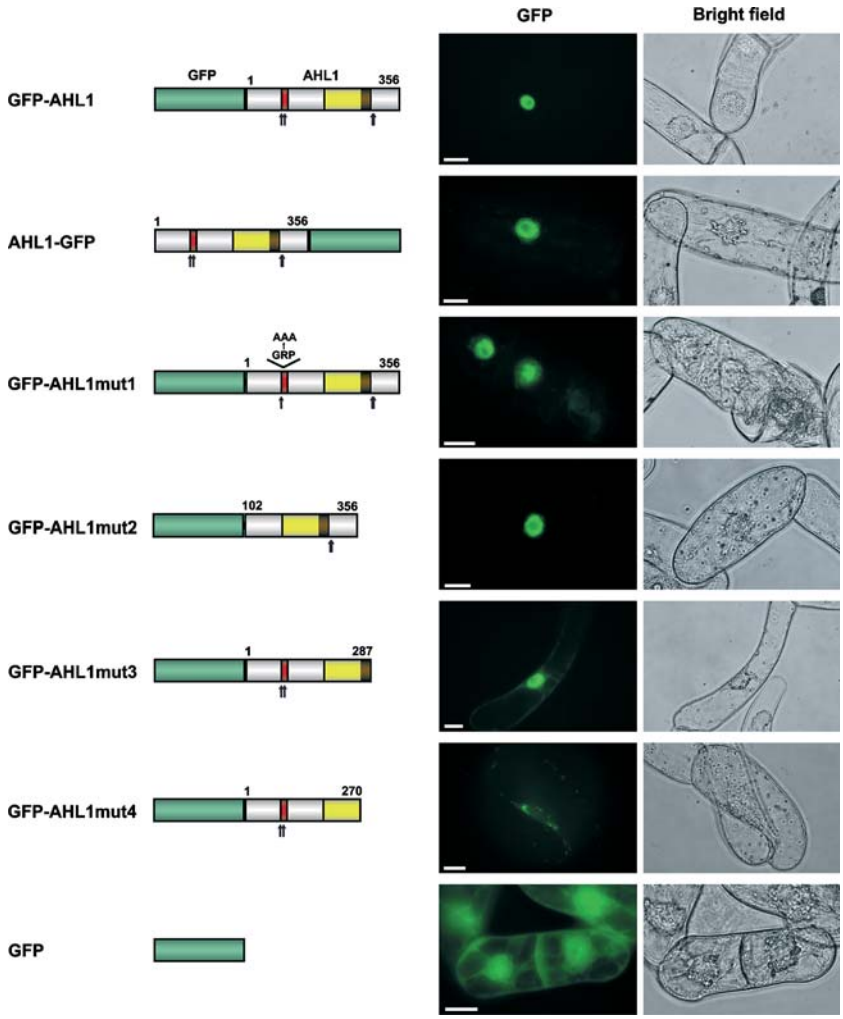

Figure 6. Effect of the AT-hook motif and PPC on the localization of GFP-AHL1. The left schematic diagrams represent the expressed proteins in cultured tobacco BY-2 cells. The AT-hook motif, PPC and hydrophobic region in PPC are indicated by red, yellow and brown boxes, respectively. The nuclear localization signals are indicated by arrows. The middle images show the GFP fluorescence used to visualize GFP fusion to AHL1 or AHL1 derivatives. The right images show bright field images of the cells. Scale bars = 20 μm.

AHM1 (Morisawa *et al*., 2000). It is also suggested that AHL1 localizes in the internal nuclear matrix. Moreover, AHL1 is abundant at the boundary between MtK4H3-positive euchromatin and DAPI-positive heterochromatin regions. Thus it is also thought that AHL1 is correlated with the determination of chromatin condensation in the nuclear matrix.

In spite of the discovery of plant nuclear matrix proteins, the localization of most of these proteins during mitosis remains unknown. Immunolocalization experiments indicated that AHL1 was localized on the chromosomal surface throughout mitosis. During mitosis, nucleoplasmic–cytoplasmic compartmentation disappears however, the chromosomal surface region has been examined by electron microscopy (Gautier *et al*., 1992a). This area persists throughout mitosis and extends a short distance from the chromosomes, but not into the surrounding cytoplasm (reviewed by Hernandez-Verdun and Gautier, 1994). The chromosomal surface region found in both animal and plant cells is co-isolated with the chromosomes after hypotonic and mechanical treatments, suggesting that it is closely bound to the chromosomes (Gautier *et al*., 1992b; Schubert *et al*., 1993).

It has been suggested that chromosomal surface proteins are involved in various roles such as chromosome organization, the formation of a barrier around the chromosomes, compartmentation of the cells during interphase-mitosis transition, and as a binding site for chromosomal passenger proteins necessary for the early processes of nuclear assembly (Hernandez-Verdun and Gautier, 1994). These proteins consist of two types of nuclear proteins one is a nuclear protein involved in the nuclear matrix and the other is the nucleolar protein found in animals (Hernandez-Verdun and Gautier, 1994). Nuclear matrix proteins such as lamin, perichromin, Ku protein and peripherin, and nucleolar proteins such as fibrillarin, perichromonucleolin and Ki-67 were all found localized on the chromosomal surface (Chaly *et al*., 1984; McKeon *et al*., 1984; Mimori *et al*., 1986; Shi *et al*., 1987; Verheijen *et al*., 1989; Glass and Gerace, 1990; Medina *et al*., 1995). In plants, fibrillarin also localizes in the nucleolus during the interphase. During mitosis, parts of these fibrillarins were also detected on the chromosomal surface and others had diffused into the cytoplasm (Medina *et al*., 1995).

To date, no plant nuclear proteins that localize on chromosomal surfaces during mitosis have been found. The subcellular distribution pattern of AHL1 during the cell cycle strongly suggests that plant species also have chromosomal surfaces, although the interphase distribution pattern in plants differs from that in animals. In *Arabidopsis* and yeast, no animal lamin homologues were found after complete genome sequencing. The role of certain kinds of nuclear proteins might depend on the organism. AHL1 might function by complementing the essential proteins of other organism. AHL1 is the first plant MAR binding protein candidate to have been identified, and is located specifically on the chromosomal surface during mitosis. The spatial localization of AHL1 during the cell cycle suggests it might have a role in the structural dynamics of chromosomes during both mitosis and the interphase. The 30 paralogues of *Arabidopsis* AHL1 might play collaborative roles in positioning chromatin within the nucleus. It is concluded therefore, that AHL1 is a novel plant MAR binding protein involved in positioning chromatin fibers in the nucleus by an AT-hook motif and PPC. Furthermore, it also potentially protects the chromosomes by covering their surfaces during mitosis or attaching to them as a passenger.

Acknowledgements

We would like to thank Dr Yasuo Niwa for providing the 35S-sGFP(S65T) plasmid; Dr Ikuo Nakamura for providing his unpublished binary vector pEBis-kH2 and plasmid SpUC19; Arabidopsis Biological Resource Center for providing the *Arabidopsis* cDNA library; Dr Akiko Terauchi and Dr Takeyuki Shimizu for their help with monoclonal antibody production; and Dr Mikako Ito and Dr Takefumi Sone for their helpful discussions. This work was supported in part by a fund (12460150) from the Ministry of Education, Culture, Sports, Science and Technology, Japan to K. F.

References

Adachi, Y., Kas, E. and Laemmli, U.K. 1989. Preferential, cooperative binding of DNA topoisomerase II to scaffold-associated regions. EMBO J. 8: 3997–4006.

Agard, D.A., Hiraoka, Y., Shaw, P. and Sedat, J.W. 1989. Fluorescence microscopy in three dimensions. Methods Cell Biol. 30: 353–377.

An, G. 1987. Binary Ti vectors for plant transformation and promoter analysis. Methods Enzymol. 153: 292–305.

Arabidopsis Genome Initiative. 2000. Analysis of the genome sequence of the flowering plant *Arabidopsis thaliana*. Nature 408: 796–815.

Aravind, L. and Landsman, D. 1998. AT-hook motifs identified in a wide variety of DNA-binding proteins. Nucleic Acids Res. 26: 4413–4421.

Ashida, H., Saito, Y., Kojima, C., Kobayashi, K., Ogasawara, N. and Yokota, A. 2003. A functional link between RuBisCO-like protein of Bacillus and photosynthetic RuBisCO. Science 302: 286–290.

Berezney, R. and Coffey, D.S. 1974. Identification of a nuclear protein matrix. Biochem. Biophys. Res. Commun. 60: 1410–1417.

Calikowski, T.T., Meulia, T. and Meier, I. 2003. A proteomic study of the *Arabidopsis* nuclear matrix. J. Cell. Biochem. 90: 361–378.

Chaly, N., Bladon, T., Setterfield, G., Little, J.E., Kaplan, J.G. and Brown, D.L. 1984. Changes in distribution of nuclear matrix antigens during the mitotic cell cycle. J. Cell Biol. 99: 661–671.

Chiu, W., Niwa, Y., Zeng, W., Hirano, T., Kobayashi, H. and Sheen, J. 1996. Engineered GFP as a vital reporter in plants. Curr. Biol. 6: 325–330.

Clough, S.J. and Bent, A.F. 1998. Floral dip: a simplified method for *Agrobacterium*-mediated transformation of *Arabidopsis thaliana*. Plant J. 16: 735–743.

Cutler, S.R., Ehrhardt, D.W., Griffitts, J.S. and Somerville, C.R. 2000. Random GFP::cDNA fusions enable visualization of subcellular structures in cells of *Arabidopsis* at a high frequency. Proc. Natl. Acad. Sci. USA 97: 3718–3723.

Dickinson, L.A., Joh, T., Kohwi, Y. and Kohwi-Shigematsu, T. 1992. A tissue-specific MAR/SAR DNA-binding protein with unusual binding site recognition. Cell 70: 631–645.

Fackelmayer, F.O., Dahm, K., Renz, A., Ramsperger, U. and Richter, A. 1994. Nucleic-acid-binding properties of hnRNP-U/SAF-A, a nuclear-matrix protein which binds DNA and RNA *in vivo* and *in vitro*. Eur. J. Biochem. 221: 749–757.

Gasser, S.M. and Laemmli, U.K. 1987. Improved methods for the isolation of individual and clustered mitotic chromosomes. Exp. Cell Res. 173: 85–98.

Gautier, T., Masson, C., Quintana, C., Arnoult, J. and Hernandez-Verdun, D. 1992a. The ultrastructure of the chromosome periphery in human cell lines. An *in situ* study using cryomethods in electron microscopy. Chromosoma 101: 502–510.

Gautier, T., Robert-Nicoud, M., Guilly, M.N. and Hernandez-Verdun, D. 1992b. Relocation of nucleolar proteins around chromosomes at mitosis. A study by confocal laser scanning microscopy. J. Cell Sci. 102 (Pt 4): 729–737.

Gerace, L. and Blobel, G. 1980. The nuclear envelope lamina is reversibly depolymerized during mitosis. Cell 19: 277–287.

Gindullis, F. and Meier, I. 1999. Matrix attachment region binding protein MFP1 is localized in discrete domains at the nuclear envelope. Plant Cell 11: 1117–1128.

Gindullis, F., Peffer, N.J. and Meier, I. 1999. MAF1, a novel plant protein interacting with matrix attachment region binding protein MFP1, is located at the nuclear envelope. Plant Cell 11: 1755–1768.

Glass, J.R. and Gerace, L. 1990. Lamins A and C bind and assemble at the surface of mitotic chromosomes. J. Cell Biol. 111: 1047–1057.

Hatton, D. and Gray, J.C. 1999. Two MAR DNA-binding proteins of the pea nuclear matrix identify a new class of DNA-binding proteins. Plant J. 18: 417–429.

He, D.C., Nickerson, J.A. and Penman, S. 1990. Core filaments of the nuclear matrix. J. Cell Biol. 110: 569–580.

Hernandez-Verdun, D. and Gautier, T. 1994. The chromosome periphery during mitosis. Bioessays 16: 179–185.

Hood, E.E., Helmer, G.L., Fraley, R.T. and Chilton, M. 1986. The hypervirulence of *Agrobacterium tumefaciens* A281 is encoded in a region of pTiBo542 outside of T-DNA. J. Bacteriol. 168: 1291–1301.

Houben, A., Demidov, D., Gernand, D., Meister, A., Leach, C.R. and Schubert, I. 2003. Methylation of histone H3 in euchromatin of plant chromosomes depends on basic nuclear DNA content. Plant J. 33: 967–973.

Huth, J.R., Bewley, C.A., Nissen, M.S., Evans, J.N., Reeves, R., Gronenborn, A.M. and Clore, G.M. 1997. The solution structure of an HMG-I(Y)-DNA complex defines a new architectural minor groove binding motif. Nat. Struct. Biol. 4: 657–665.

Izaurralde, E., Kas, E. and Laemmli, U.K. 1989. Highly preferential nucleation of histone H1 assembly on scaffold-associated regions. J. Mol. Biol. 210: 573–585.

Kieber, J.J., Rothenberg, M., Roman, G., Feldmann, K.A. and Ecker, J.R. 1993. CTR1, a negative regulator of the ethylene response pathway in *Arabidopsis*, encodes a member of the raf family of protein kinases. Cell 72: 427–441.

Kikuchi, S., Satoh, K., Nagata, T., Kawagashira, N., Doi, K., Kishimoto, N., Yazaki, J., Ishikawa, M., Yamada, H., Ooka, H., Hotta, I., Kojima, K., Namiki, T., Ohneda, E., Yahagi, W., Suzuki, K., Li, C.J., Ohtsuki, K., Shishiki, T., Otomo, Y., Murakami, K., Iida, Y., Sugano, S., Fujimura, T., Suzuki, Y., Tsunoda, Y., Kurosaki, T., Kodama, T., Masuda, H., Kobayashi, M., Xie, Q., Lu, M., Narikawa, R., Sugiyama, A., Mizuno, K., Yokomizo, S., Niikura, J., Ikeda, R., Ishibiki, J., Kawamata, M., Yoshimura, A., Miura, J., Kusumegi, T., Oka, M., Ryu, R., Ueda, M., Matsubara, K., Kawai, J., Carninci, P., Adachi, J., Aizawa, K., Arakawa, T., Fukuda, S., Hara, A., Hashidume, W., Hayatsu, N., Imotani, K., Ishii, Y., Itoh, M., Kagawa, I., Kondo, S., Konno, H., Miyazaki, A., Osato, N., Ota, Y., Saito, R., Sasaki, D., Sato, K., Shibata, K., Shinagawa, A., Shiraki, T., Yoshino, M. and Hayashizaki, Y. 2003. Collection, mapping, and annotation of over 28,000 cDNA clones from japonica rice. Science 301: 376–379.

Ludérus, M.E., de Graaf, A., Mattia, E., den Blaauwen, J.L., Grande, M.A., de Jong, L. and van Driel, R. 1992. Binding of matrix attachment regions to lamin B1. Cell 70: 949–959.

Ludérus, M.E., den Blaauwen, J.L., de Smit, O.J., Compton, D.A. and van Driel, R. 1994. Binding of matrix attachment regions to lamin polymers involves single-stranded regions and the minor groove. Mol. Cell Biol. 14: 6297–6305.

Masuda, K., Xu, Z.J., Takahashi, S., Ito, A., Ono, M., Nomura, K. and Inoue, M. 1997. Peripheral framework of carrot cell nucleus contains a novel protein predicted to exhibit a long alpha-helical domain. Exp. Cell Res. 232: 173–181.

McKeon, F.D., Tuffanelli, D.L., Kobayashi, S. and Kirschner, M.W. 1984. The redistribution of a conserved nuclear envelope protein during the cell cycle suggests a pathway for chromosome condensation. Cell 36: 83–92.

McNulty, A.K. and Saunders, M.J. 1992 Purification and immunological detection of pea nuclear intermediate filaments: evidence for plant nuclear lamins. J. Cell Sci. 103: 407–414.

Medina, F.J., Cerdido, A. and Fernandez-Gomez, M.E. 1995. Components of the nucleolar processing complex (Pre-rRNA, fibrillarin, and nucleolin) colocalize during mitosis and are incorporated to daughter cell nucleoli. Exp. Cell Res. 221: 111–125.

Meier, I., Phelan, T., Gruissem, W., Spiker, S. and Schneider, D. 1996. MFP1, a novel plant filament-like protein with affinity for matrix attachment region DNA. Plant Cell 8: 2105–2115.

Merdes, A., Ramyar, K., Vechio, J.D. and Cleveland, D.W. 1996. A complex of NuMA and cytoplasmic dynein is essential for mitotic spindle assembly. Cell 87: 447–458.

Mimori, T., Hardin, J.A. and Steitz, J.A. 1986. Characterization of the DNA-binding protein antigen Ku recognized by autoantibodies from patients with rheumatic disorders. J. Biol. Chem. 261: 2274–2278.

Minguez, A. and Moreno Diaz de la Espina, S. 1993. Immunological characterization of lamins in the nuclear matrix of onion cells. J. Cell Sci. 106: 431–439.

Mirkovitch, J., Mirault, M.E. and Laemmli, U.K. 1984. Organization of the higher-order chromatin loop: specific DNA attachment sites on nuclear scaffold. Cell 39: 223–232.

Morisawa, G., Han-Yama, A., Moda, I., Tamai, A., Iwabuchi, M. and Meshi, T. 2000. AHM1, a novel type of nuclear matrix-localized, MAR binding protein with a single AT hook and a J domain-homologous region. Plant Cell 12: 1903–1916.

Nakai, K. and Kanehisa, M. 1992. A knowledge base for predicting protein localization sites in eukaryotic cells. Genomics 14: 897–911.

Olins, A.L. and Olins, D.E. 1974. Spheroid chromatin units (v bodies). Science 183: 330–332.

Penman, S. 1995. Rethinking cell structure. Proc. Natl. Acad. Sci. USA 92: 5251–5257.

Pienta, K.J., Getzenberg, R.H. and Coffey, D.S. 1991. Cell structure and DNA organization. Crit. Rev. Eukaryot. Gene Expr. 1: 355–385.

Reeves, R. and Nissen, M.S. 1990. The AT-DNA-binding domain of mammalian high mobility group I chromosomal proteins. A novel peptide motif for recognizing DNA structure. J. Biol. Chem. 265: 8573–8582.

Sambrook, J., Fritsch, E.F. and Maniatis, T. 1989. Molecular Cloning: A Laboratory Manual, 2nd edn. Cold Spring Harbor Laboratory Press, Cold Spring Harbor.

Shi, L.J., Ni, Z.M., Zhao, S., Wang, G. and Yang, Y. 1987. Involvement of a nucleolar component, perichromonucleolin, in the condensation and decondensation of chromosomes. Proc. Natl. Acad. Sci. USA 84: 7953–7956.

Schubert, I., Dolezel, J., Houben, A., Scerthan, H. and Wanner, G. 1993. Refined examination of plant metaphase chromosome structure at different levels made feasible by new isolation methods. Chromosoma 102: 96–101.

Strahl, B.D. and Allis, C.D. 2000. The language of covalent histone modifications. Nature 403: 41–45.

Sumner, A.T. 1996. The distribution of topoisomerase II on mammalian chromosomes. Chromosome Res. 4: 5–14.

Swedlow, J.R., Sedat, J.W. and Agard, D.A. 1993. Multiple chromosomal populations of topoisomerase II detected *in vivo* by time-lapse, three-dimensional wide-field microscopy. Cell 73: 97–108.

Tsutsui, K., Tsutsui, K., Okada, S., Watarai, S., Seki, S., Yasuda, T. and Shohmori, T. 1993. Identification and characterization of a nuclear scaffold protein that binds the matrix attachment region DNA. J. Biol. Chem. 268: 12886–12894.

van Drunen, C.M., Oosterling, R.W., Keultjes, G.M., Weisbeek, P.J., van Driel, R. and Smeekens, S.C.M. 1997. Analysis of the chromatin domain organisation around the plastocyanin gene reveals an MAR-specific sequence element in *Arabidopsis thaliana*. Nucleic Acids Res. 25: 3904–3911.

van Holde, K. and Zlatanova, J. 1995. Chromatin higher order structure: chasing a mirage? J. Biol. Chem. 270: 8373–8376.

Verheijen, R., Kuijpers, H.J., van Driel, R., Beck, J.L., van Dierendonck, J.H., Brakenhoff, G.J. and Ramaekers, F.C. 1989. Ki-67 detects a nuclear matrix-associated proliferation-related antigen. II. Localization in mitotic cells and association with chromosomes. J. Cell Sci. 92 (Pt 4): 531–540.

von Kries, J.P., Buck, F. and Stratling, W.H. 1994. Chicken MAR binding protein p120 is identical to human heterogeneous nuclear ribonucleoprotein (hnRNP) U. Nucleic Acids Res. 22: 1215–1220.

Wako, T., Fukuda, M., Furushima-Shimogawara, R., Belyaev, N.D. and Fukui, K. 2002. Cell cycle-dependent and lysine residue-specific dynamic changes of histone H4 acetylation in barley. Plant Mol. Biol. 49: 645–653.

Xia, Y., Nikolau, B.J. and Schnable, P.S. 1997. Developmental and hormonal regulation of the *Arabidopsis* CER2 gene that codes for a nuclear-localized protein required for the normal accumulation of cuticular waxes. Plant Physiol. 115: 925–937.

Yu, W. and Moreno Diaz de la Espina, S. 1999. The plant nucleoskeleton: ultrastructural organization and identification of NuMA homologues in the nuclear matrix and mitotic spindle of plant cells. Exp. Cell Res. 246: 516–526.

Zhao, K., Kas, E., Gonzalez, E. and Laemmli, U.K. 1993. SAR-dependent mobilization of histone H1 by HMG-I/Y *in vitro*: HMG-I/Y is enriched in H1-depleted chromatin. EMBO J. 12: 3237–3247.